NJC

Accepted Manuscript

This is an *Accepted Manuscript*, which has been through the Royal Society of Chemistry peer review process and has been accepted for publication.

Accepted Manuscripts are published online shortly after acceptance, before technical editing, formatting and proof reading. Using this free service, authors can make their results available to the community, in citable form, before we publish the edited article. We will replace this *Accepted Manuscript* with the edited and formatted *Advance Article* as soon as it is available.

You can find more information about *Accepted Manuscripts* in the Information for Authors.

Please note that technical editing may introduce minor changes to the text and/or graphics, which may alter content. The journal's standard Terms & Conditions and the Ethical guidelines still apply. In no event shall the Royal Society of Chemistry be held responsible for any errors or omissions in this *Accepted Manuscript* or any consequences arising from the use of any information it contains.

ROYAL SOCIETY OF CHEMISTRY

www.rsc.org/njc

Journal Name

ARTICLE

Phase-Pure Fabrication and Shape Evolution Studies of SnS Nanosheets

Received 00th January 20xx,
Accepted 00th January 20xx

DOI: 10.1039/x0xx00000x

www.rsc.org/

Malik Dilshad Khan,[a] Javeed Akhtar,[b] Mohammad Azad Malik,[a, c] Masood Akhtar,[a, c] and Neerish Revaprasadu*[a]

Phase pure SnS nanosheets were synthesized by hot injection method from a new single molecular precursor (SMP), dibutyl-*bis*(piperidinedithiocarbamato)tin(IV) in oleylamine at 230 °C. The tin complex was characterized by single crystal X-ray crystallography, nuclear magnetic resonance, thermogravimetric and microelemental analysis. The complex is thermally stable up to 260 °C, after which it decomposes in a single step with a major mass loss between 260 °C to 300 °C. The thermolysis of as-prepared precursor was carried out in oleylamine between 190-230 °C. The formation and shape evolution of SnS was investigated using high resolution electron microscopy. The mechanism of time dependent growth of the SnS from spherical particles into nanosheets is proposed.

Introduction

The distinctive optical, electrical and magnetic properties of metal sulfide nanostructures have potential applications in biomedicine, optoelectronic devices and catalysis.[1-6] Therefore phase pure and size controllable synthesis of metal sulfides with desired optical and electronic properties are important for both fundamental studies and technological applications.[7] Tin sulfides are a class of IV–VI semiconductors which have many phases such as SnS, Sn_2S_3, Sn_3S_4, Sn_4S_5 and SnS_2[8] SnS is a narrow band gap material with both an indirect and a direct band gap (1.1 eV and 1.3 eV), whereas SnS_2 is an important mid-band gap (2.2-2.35 eV) semiconductor.[3] The earth abundant nature, low toxicity, chemical stability, band gap position and low cost of SnS makes it an attractive photovoltaic material.[9-12] The use of SnS as an anode material for lithium ion batteries has also been reported.[13-16] Layered 2D materials have attracted attention in recent years due to their anisotropic properties which are dependent on thickness of the sheets.[17-19] There has been recent focus on the synthesis of ultrathin two-dimensional (2D) SnS materials which have demonstrated unique electronic properties.[20-24] For example the migration of electrons in 2D materials make them excellent candidates in electrodes, conducting films and photovoltaic devices.[9] Most of the synthetic methodologies involve the use of dual source e.g tin hydroxide/thioacetamide in various coordinating and non-coordinating solvents.[25-28] A variation in the reaction conditions (reaction temperature and Sn/S molar ratio) gave SnS nanocrystals with different shapes and sizes. The synthesis of size tunable SnS nanoparticles in the form of smaller spheres and larger tetrahedrons have been reported using the hot injection method.[13-29] Despite numerous investigations on the properties of layered materials, a systematic study on formation mechanism of these materials has not yet been demonstrated. It is important to investigate the mechanism of nanosheet formation to effectively utilize 2D nanostructures in applications by tuning the thickness and size of sheets. We have reported the synthesis of single source precursors and their use to deposit semiconductor thin films or nanoparticles.[30-37] Herein, we report the synthesis of a new organotin complex, its X-ray single crystal structure determination and its use as a single molecular precursor for SnS nanostructures. Our study also shows how the SnS nanosheets evolve from spherical nanoparticles as the reaction proceeds.

Experimental

Materials

Oleylamine (technical grade), piperidine, carbon disulfide, sodium hydroxide, and dibutyl tin dichloride were purchased from Sigma Aldrich and were used as such.

Synthesis of dibutyl *bis*(piperidinedithiocarbamato)tin(IV)

The ligand was synthesized as reported in the literature.[8] Briefly the reaction of piperidinedithiocarbamatosodium (3.0 g, 18.6 mmol) in ethanol with dibutyltin dichloride (2.8 g, 9.3 mmol) in ethanol at room temperature for 30 minutes resulted in the formation of the product. The white solid was recrystallized using ethanol and chloroform (1:1) mixture which yielded colorless crystalline needles. Yield, 4.0 g (77 %). M.pt: 94-95 °C. Elemental analysis: Calc. for $C_{20}H_{38}N_2S_4Sn$: C, 43.39; H, 6.87; N, 5.06 %. Found: C, 43.49; H, 6.73; N, 5.19 %. ^{1}HNMR (δ/ppm): N(C**H**$_2$)$_2$ 3.59 m, N(CH$_2$**C**H$_2$)$_2$ 1.40 m, N(CH$_2$CH$_2$)$_2$C**H**$_2$ 1.79 m, Sn-CH$_2$CH$_2$CH$_2$CH$_3$, 0.64–1.1 m, 0.23 t.

[a] Department of Chemistry, University of Zululand, Private bag X1001, Kwa-Dlangezwa 3880. Address here.
[b] Polymers and Materials Synthesis (PMS) Lab, Department of Physics, COMSATS, Institute of Information Technology (CIIT), Chak Shahzad, Islamabad Pakistan.
[c] School of Materials, The University of Manchester, Oxford Road, Manchester, M13 9PL, UK..

Synthesis of SnS nanosheets

Briefly 8.0 g (30 mmol) of oleylamine (OLA) was placed in three-neck round bottom flask and heated to 120 °C under vacuum to degas and remove residual water. The flask was flushed with nitrogen and then heated to 230 °C, where the temperature was maintained for 30 minutes. Dibuty-bis(piperidinedithiocarbamato)tin(IV) (0.4 g, 7.5 mmol) was dissolved in TOP (2.0 ml) and then rapidly injected into the coordinating solvent. The color of solution changes instantly from light yellow to black-brown, indicating the formation of nanoparticles. Aliquots were taken after different time intervals during the reaction. The initial sample was removed after two minutes of the reaction. Acetone was used as precipitating agent in each aliquot, which was then centrifuged to separate the nanoparticles. The supernatant was subsequently discarded and the precipitate was redispersed in a hexane acetone mixture and followed by several washings to obtain the pure nanoparticles. The reaction was stopped after 30 mins.

Characterization of SnS NPs

The morphology and particle size of the SnS samples were characterized by TEM (JEOL 1010) with an accelerating electrical potential of 100 kV. The X-ray diffraction was performed using a Bruker AXS D8 diffractometer coupled with CuK_{α} radiation (λ = 1.5406 Å) as target materials at 40 kV, 40 mA in a 2θ range from 10° to 80°. The data collected were used to determine the lattice parameter, crystallite size and crystalline phase. Samples for XRD were repetitively washed with excess acetone to ensure a complete removal of capping agent and thereafter dried at room temperature.

Single crystal X-ray structure

Single-crystal X-ray diffraction data for the complex was collected using graphite monochromated Mo-Kα radiation (λ = 0.71073 A) on a Bruker APEX diffractometer. The structure was solved by direct methods and refined by full-matrix least squares[38]on F2. All non-H atoms were refined anisotropically. Hydrogen atoms were included in calculated positions, assigned isotropic thermal parameters and allowed to ride on their parent carbon atoms. All calculations were carried out using the SHELXTL package.[39] The refined data of the crystals as follows. Empirical formula; C20 H38 N2 S4 Sn; Formula weight = 553.45; Monoclinic; C2/c; a = 19.852(2) Å, b = 6.7979(6) Å, c = 19.7407(17) Å; α= 90°, β= 100.635(4)°, γ = 90°; V = 2618.3(4) Å3; Z = 4; D =1.404 Mg/m3; Independent reflections = 2532 [R(int) = 0.0263]; Refinement method = Full-matrix least-squares on F2; Data / restraints / parameters =2532 / 0 / 124, Goodness-of-fit on F2 = 1.091; Final R indices = [I>2sigma(I)],R1 = 0.0236, wR2 = 0.0581; R indices (all data) = R1 = 0.0252, wR2 = 0.0591; Largest diff. peak and hole = 1.008 and -0.622 e.Å-3. The single crystal structure of the complex belongs to monoclinic crystal system with space group C2/c, and overall geometry is skewed trapezoidal bipyramid as shown in Fig. 1. There are four sulphur coordinating atoms and two carbon centres demonstrating six coordination number. Two of Sn-S bond lengths, Sn1-S1 and Sn1-S1A are 2.529 Å, which are comparatively shorter than Sn1-S2 and Sn1-S2A (2.919 Å). The crystal structure analysis shows that short thioureide C-N distance is 1.333(2) suggesting partial double bond characters. These results are comparable with the structure reported in the literature.[40,41]

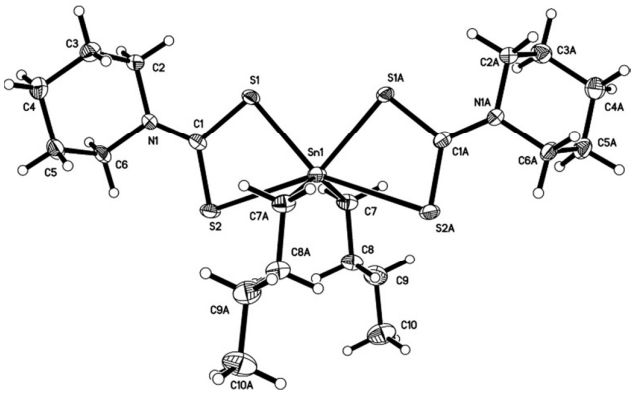

Fig. 1. Selected bond lengths [Å] and angles [°] for crystal structure: S(1)-Sn(1) 2.5298(5), S(2)-Sn(1) 2.9194(5), Sn(1)-C(7)#1 2.147(2), Sn(1)-S(1)#1 2.5299(5), Sn(1)-S(2)#1 2.9194(5),C(7)#1-Sn(1)-C(7) 143.48(11), C(7)#1-Sn(1)-S(1) 101.69(6),C(7)-Sn(1)-S(1) 105.33(5), C(7)#1-Sn(1)-S(1)#1 105.33(5),C(7)-Sn(1)-S(1)#1 101.69(6), S(1)-Sn(1)-S(1)#1 83.66(2),C(7)#1-Sn(1)-S(2)#1 85.46(6), C(7)-Sn(1)-S(2)#183.78(6),S(1)Sn(1)S(2)#1149.202(14),S(1)#1Sn(1)S(2)#165.603 (14), C(7)#1-Sn(1)-S(2)83.78(6),C(7)-Sn(1)-S(2) 85.46(6), S(1)-Sn(1)-S(2)

Results and discussion

Dibutyl bis(piperidinedithiocarbamato)tin(IV) was synthesized by reacting piperidinedithiocarbamatosodium with dibutyltin dichloride in ethanol. The tin complex was then thermolysed in different capping groups using the hot injection route. It was observed that when precursor was injected in tri–n-octylphosphineoxide (TOPO), dodecane thiol (DDT) or oleic acid (OLAc) using trioctylphosphine (TOP) as dispersion medium, there was no evidence of decomposition even at an elevated temperature of 250 °C. However, when the precursor was injected in oleylamine (OLA) there was partial decomposition even at a lower temperature of 190 °C. Similar behavior was shown by hexadecylamine (HDA), which suggests that the primary amines facilitate the decomposition of this precursor. We decided to use the OLA as a capping agent, with an optimum temperature of 230 °C.

The thermal stability of metal complex in solid state was studied by thermogravimetric analysis in the range of 30 °C to 500 °C at heating rate of 10 °C in nitrogen atmosphere. The complex is thermally quite stable and there is no sign of any mass loss before 260 °C, after which there is a single step decomposition with major mass loss in the range of 260 °C to 300 °C as-depicted in Fig. S1 (supplementary data). The solid residue left after decomposition was ca. 18 % of the original mass, whereas the theoretical mass calculated for SnS is 27.2 %. The weight loss is more than what is required for formation of SnS theoretically. The experimental weight loss do not correspond to any oxide of tin, elemental sulphur or tin. So it can be presumed that some sublimation of precursor occurs during TGA analysis due to

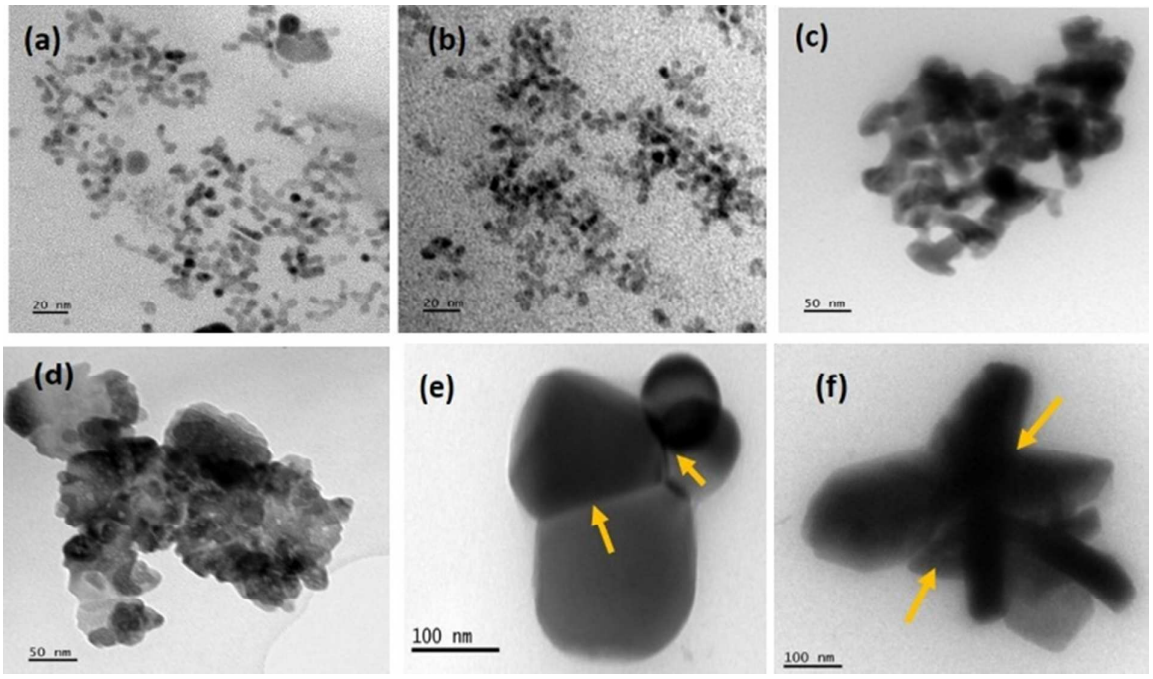

Fig. 2. TEM images of aliquots showing the formation of SnS nanoparticles, highlighting initial nucleation (a,b) after 2 minutes reaction time, agglomeration (c-f) after 5 minutes.

which the accurate value is difficult to obtain. In order to check the nature of residue, a small quantity of precursor was added in ceramic combustion boat and it was slowly heated to 450 °C in carbolite tube furnace under argon atmosphere for one hour. The XRD pattern of the residue shown in Fig. S1a (supplementary data) corresponded to orthorhombic SnS (ICDD # 00-039-0354).

The formation of SnS nanosheets

The thermolysis in oleylamine was carried out at 230 °C and the aliquots were collected at various time intervals during the course of reaction to monitor the shape transition by TEM. The first aliquot, collected after 2 minutes, show spherical nanoparticles or seeds formed in the 5 to 10 nm size range (Fig. 2a, b). These nanoparticles appear to form a network through attachment. After 5 minutes of reaction the nanoparticles start to aggregate (Fig. 2c-f). The particles align themselves at certain planes and attach to each other as shown by the arrows in Fig. (2e-f). The oleylamine probably facilitates the fusion of the particles through adsorption onto specific facets.[42] Further heating transforms the aggregates into regular cube shaped particles as shown in the TEM images in Fig. 4. The cubes formed after 10 minutes appear transparent (Fig. 4a). After 15 minutes we observe evidence of lateral growth where the cubic crystallites appear to assemble or 'stack up' in a lateral direction (Fig. 4b). It seems that the first cubic layer acted as a template for the formation of successive layers, which suggests that the growth occurs first along the horizontal direction followed by the vertical plane. The cubes become opaque after successive growth of layers (Fig. 4c). The cubic crystallites are randomly dispersed with some (shown by arrows in Fig. 4d-f) showing a tendency to assemble forming sheet-like structures.

Further evidence of the growth transition is shown in Fig. S2 (supplementary data). The cubic sheets formed initially are quite thin as transparency of these nanosheets with respect to electron beam increases. They have a tendency to buckle and fold Fig. S2 (supplementary data). This mechanism then facilitates the vertical growth of the particles. Vaughn *et al.*[25] observed similar behavior of SnSe sheets which also grew laterally and then vertically through attachment to the nanosheet template. However, they could not identify the factors that influence the vertical growth.

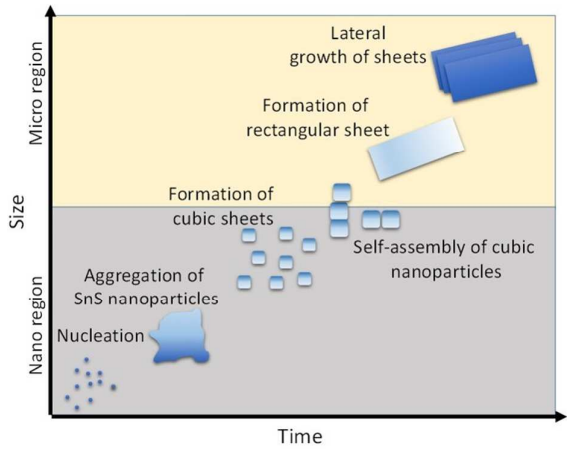

Fig. 3. Pictorial representation of different stages of the growth of SnS nanosheet.

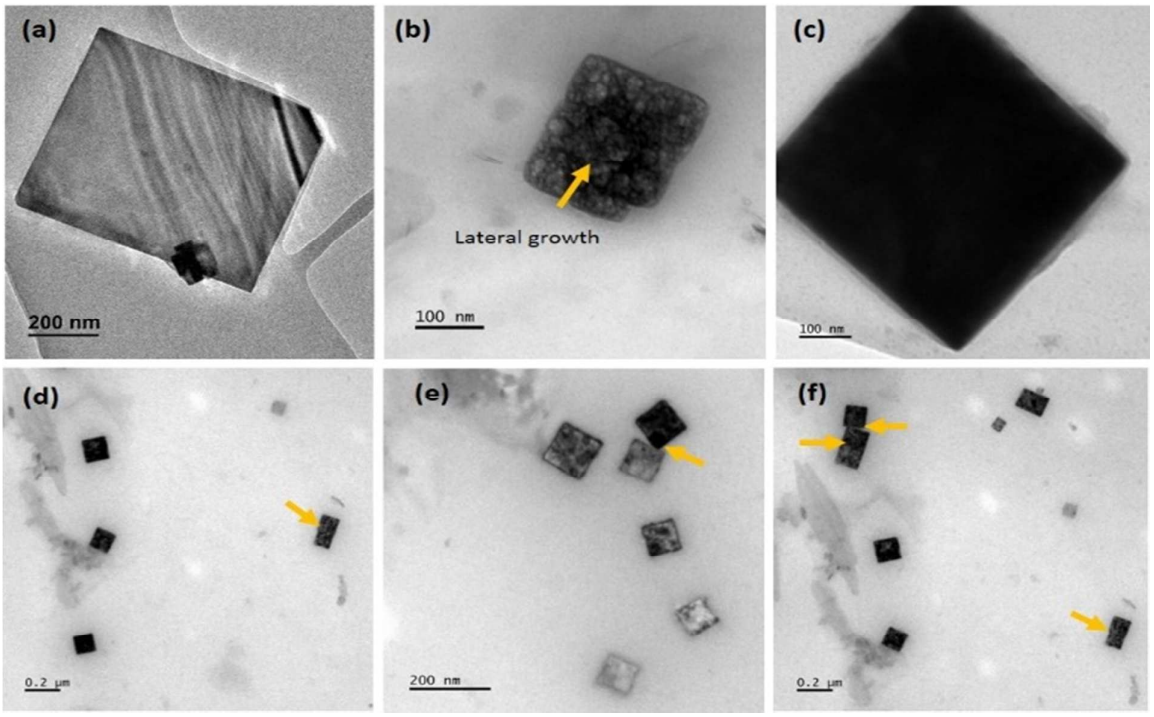

Fig. 4. TEM images of aliquots showing the formation of transparent cubic sheet (a) after 10 min and lateral growth (b-f) after 15 min.

Interestingly the lateral growth does not stop here, after 20 minutes the cubic sheet- like particles then assemble in a precise manner as shown in Fig. 5 (a,b). Transparent rectangular sheets are formed after 25 minutes (Fig. 5c) which become darker and thicker after 30 minutes (Fig. 5d). The rectangular SnS nanosheet shown in Fig. 5d have a length of 998 nm and breadth of 465 nm. The mechanism for the attachment of the cubic sheets (3-D) to form the horizontal sheets (2-D) follows through an oriented attachment mechanism.[27,28] OLA allows the nanosheets to form through the alignment and coalescence of neighbouring nanostructures by eliminating the capping agent boundaries. We observe the alignment and fusion of the two nanocubes in Fig. S3 (supplementary data).

The growth of the nanosheets from the initially formed particles follows four steps, nucleation, aggregation, coalescence and finally assembly through oriented attachment. We have depicted the growth of the SnS nanosheets as a function of time in the schematic illustration Fig.3. The growth is similar to that of hierarchal SnS_2 nanoplates, which assemble as a function of L-cys concentration.[29]

This low temperature kinetic growth is controlled by the release of S^{2-} ions in solution. In our work, the high temperature used means that the growth is thermodynamically controlled. The decomposition of the precursor as a function of reaction time results in a change of ratio of Sn^{2+} and S^{2-} ions in the oleylamine matrix. Any small change in ratio of the ions to the capping group has an effect on the surface free energy resulting in anisotropic growth. The growth mechanism is influenced by the energy which surfactant molecules adhere to the nanocrystals. The adhesion energy must facilitate dynamic solvation whereby the surfactant is able to exchange on and off the growing crystals while still allowing regions of the nanocrystal surface to grow. Dynamic adsorption and desorption processes occur whereby the surface atoms and ligands results in the reorganization of the particle surfaces to minimize the surface energy. This accounts for the formation of the initial cubic structures of SnS. The assembly and fusion of the cubic

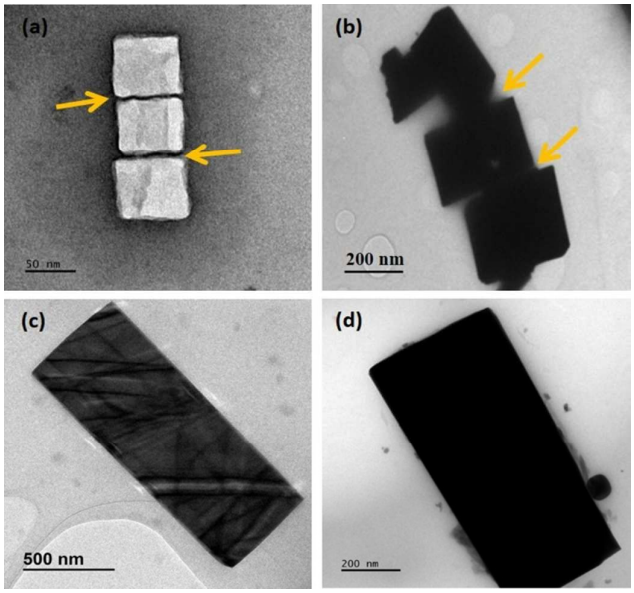

Fig. 5. TEM images showing alignment assembly of SnS cubes (a-b) after 20 minutes, (c) formation of SnS nanosheets after 25 minutes and finally (e) thicker nanosheets after 30 minutes.

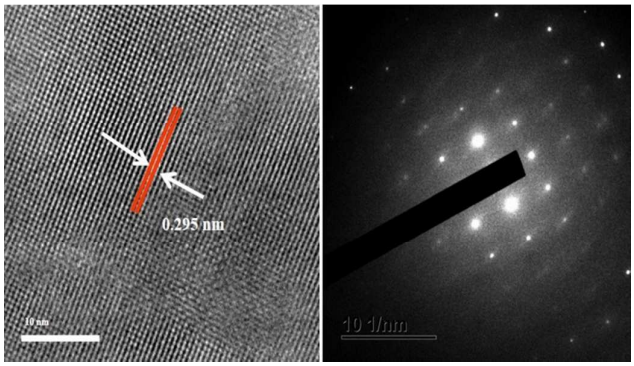

Fig. 6. (a) HRTEM image of SnS nanosheet (25 min.) and (b) SAED pattern.

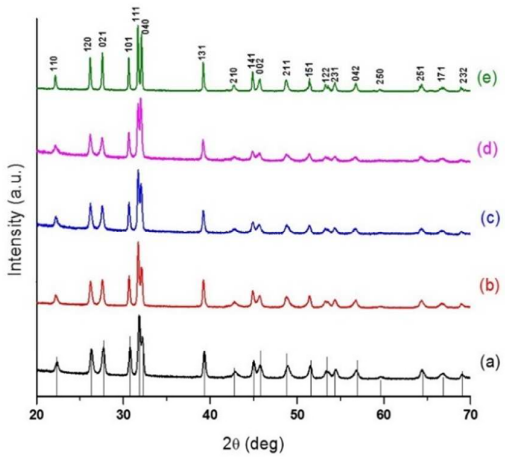

Fig. 7. XRD pattern of SnS from nanoparticles to sheet formation (Ordered from (a) to (e) with increasing time)

structures to form the rectangular sheets which also stack up vertically is due to the oriented attachment mechanism.

The SnS nanosheets are highly crystalline as shown by the lattice fringes in the HRTEM image and well defined spots in the SAED pattern (Fig. 6). This is in contrast to the SAED pattern of the particles in the early stage of the reaction (10 min. sample) which showed circular rings, evidence of poorly crystalline particles Fig. S4 (supplementary data). The lattice spacing of 0.295 nm in the HRTEM can be indexed to the (101) plane of the orthorhombic phase of SnS as shown in Fig. 6. The major X-ray diffraction peaks are indexed as (110), (120), (021), (101), (111), (040), (131) and (141) planes of orthorhombic SnS nanocrystals with (ICDD# 00-039-0354) as shown in Fig. 7. There is no change in phase as the reaction proceeds with time, however there is a change in the intensity of the peaks. The expansion of XRD portion in region of 31° to 33° for various nanoparticles thickness and time as shown in Fig. S5 (supplementary data) shows an increase in the intensity of the (040), becoming sharper and more distinct, with increasing time interval. The change in full width at half maximum of XRD peaks of nanoparticles analyzed at different reaction time clearly indicates the formation of larger particles with increasing the reaction time. The oxidation state of Sn is +2 as peaks match well with SnS phase only and there is no transformation in phase while forming the nanosheets. It may be noted that the precursor has Sn in +4 state but it changes to +2 state after formation of nanoparticles and sheets. The EDX result also show the presence of Sn and S in almost 1:1 ratio, indicating good stoichiometry of SnS nanoparticles Fig. S6 (supplementary data). The formation of Sn^{2+} is probably due to strong reductive environment of oleylamine, an excess of which favours SnS formation. The oleylamine has a duel function of a surface capping group and also providing a reductive environment for the decomposition of the precursor.[42,43]

Conclusions

We have reported the synthesis of a new organotin complex which was used as a single molecular precursor to grow SnS nanostructures in oleylamine at 230 °C. The formation and shape transformation of SnS was investigated by collecting aliquots at different time intervals. Nearly spherical SnS nanoparticles were formed after two minutes which changed to 'clumps' and eventually nanocubes then to nanosheets as the reaction time increases. These nanosheets undergo stacking to form multi-layer 2D structures. A plausible mechanism for the formation of 2D nanosheets is proposed.

Acknowledgements

NR thanks the National Research Foundation (NRF), South Africa through the South African Research Chair Initiative (SARChI) program for financial support. JA thanks the COMSATS Institute of Information Technology (CIIT) Islamabad for funding the project "Phase and Composition Controlled Deposition of Copper Sulfide Nanostructures", grant number 16-61/CRGP/CIIT/IBD/12/943 and also acknowledges financial assistance from the Higher Education Commission.

Notes and references

1. Z. Fan, X. Huan, C. Tan and H. Zhang, *Chem. Sci.*, 2015, **6**, 95.
2. Y. M. Han, J. Zhao, M. Zhou, X. X. Jiang, H. Q. Leng and L.F. Li, *J. Mater. Chem. A*, 2015, **3**, 4555.
3. S. G. Hickey, C. Waurisch, B. Rellinghaus and A. Eychmüller, *J. Am. Chem. Soc.*, 2008, **130**, 14978.
4. T. Jiang, and G. A. Ozin, *J. Mater. Chem.,* 1998, **8**, 1099.
5. C. H. Lai, M. Y. Lu and L. J. Chen, *J. Mater. Chem.*, 2012, **22**, 19.
6. X. Liu, Y. Li, B. Zhou, X. Wang, A. N. Cartwright and M. T. Swihart, *Chem. Mater.,* 2014, **26**, 3515.
7. K. Ramasamy, M. A. Malik, N. Revaprasadu and P. O'Brien, *Chem. Mater.,* 2013, **25**, 3551.
8. K. Ramasamy, V. L. Kuznetsov, K. Gopal, M. A. Malik, J. Raftery, P. P.Edwards and P. O'Brien, *Chem. Mater.,* 2013, **25**, 266.
9. M. Y. Sun, J. Yang, T. Lin and X. W. Du, *RSC Advances,* 2012, **2**, 7824.
10. G. Xiao, Y. Wang, J. Ning, Y. Wei, B. Liu, W. W. Yu, G. Zou and B. Zou, *RSC Advances,* 2013, **3**, 8104.

11. S. Alexandros, M. S. Jason, A. C. Christopher, G. C. Andrew, S. G. Patrick and A. R. W. Andrew, *Nanotechnology,* 2010, **21**, 185202.
12. Z. Wang, S. Qu, X. Zeng, J. Liu, C. Zhang, F. Tan, L. Jin and Z. Wang, *J. Alloy. Compd.,* 2009, **482**, 203.
13. Z. Deng, D. Han and Y. Liu, *Nanoscale,* 2011, **3**, 4346.
14. Y. Zhang, J. Lu, S. Shen, H. Xu and Q. Wang, *Chem. Commun.,* 2011, **47**, 5226.
15. D. J. Lewis, P. Kevin, O. Bakr, C. A. Muryn, M. A. Malik and P. O'Brien, *Inorg. Chem. Front.,* 2014, **1**, 577.
16. K. Aso, A. Hayashi and M. Tatsumisago, *Cryst. Growth Des.,* 2011, **11**, 3900.
17. C. Ataca, H. Şahin and S. Ciraci, *J. Phys. Chem. C,* 2012, **116**, 8983.
18. M. Xu, T. Liang, M. Shi and H. Chen, *Chem. Rev.,* 2013, **113**, 3766.
19. D. J. Lewis, P. Kevin, O. Bakr, C. A. Muryn, M. A. Malik and P. O'Brien, *Inorg. Chem. Front*., 2014, **1**, 577.
20. J. H. Ahn, M. J. Lee, H. Heo, J. H. Sung, K. Kim, H. Hwang, and M. H. Jo, *Nano Lett.,* 2015, **15**, 3703.
21. S. Biswas, S. Kar and S. Chaudhuri, *Appl. Surf. Sci.,* 2007, **253**, 9259.
22. J. Ning, K. Men, G. Xiao, L. Wang, Q. Dai, B. Zou, B. Liu and G. Zou, *Nanoscale,* 2010, **2**, 1699.
23. S. Chaki, M. Chaudhary and M. P. Deshpande, *J Therm Anal Calorim,* 2015, **120**, 1261.
24. A. K. Geim, and K. S. Novoselov, *Nat Mater,* 2007, **6**, 183.
25. D. D. Vaughn, S. I. In and R. E. Schaak, *ACS Nano,* 2011, **5**, 8852.
26. J. Zhang, F. Huang and Z. Lin, *Nanoscale,* 2010, **2**, 18.
27. J. Zai, X. Qian, K. Wang, C. Yu, L. Tao, Y. Xiao and J. Chen, *CrystEngComm,* 2012, **14**, 1364.
28. Y. Tao, X. Wu, W. Wang and J. Wang, *J. of Mater. Chem. C,* 2015, **3**, 1347.
29. X. Zhang, L. Yang, Y. Jiang, B. -B. Yu, Y. G. Zou, Y. Fang, J. S. Hu and L. J. Wan, *Asian J.Chem.,* 2013, **8**, 2483.
30. N. Revaprasadu, M.A. Malik, P. O'Brien, and G. Wakefield, *J. Mater. Res.*, 1999, **14,** 3237.
31. M.A. Malik, M. Motevalli, and P. O'Brien, *Inorg. Chem.*, 1995, **34,** 6223.
32. M.A. Malik, M. Motevalli, J.R. Walsh, and P. O'Brien, *Organometallics*, 1992, **11,** 3136.
33. A.A. Memon, M. Afzaal, M.A. Malik, C.Q. Nguyen, P. O'Brien, and J. Raftery, *Dalton Trans.*, 2006, **37,** 4499.
34. D. Binks, S. Bant, D. West, P. O'brien, and M. Malik, *J. Mod. Optic.*, 2003, **50,** 299.
35. C.Q. Nguyen, A. Adeogun, M. Afzaal, M.A. Malik, and P. O'Brien, *Chem. Commun.*, 2006, **20,** 2182.
36. M.A. Malik, M. Motevalli, T. Saeed, and P. O'Brien, *Adv. Mater.*, 1993, **5,** 653.
37. A. Panneerselvam, C.Q. Nguyen, M.A. Malik, P. O'Brien, and J. Raftery, *J. Mater. Chem.*, 2009, **19,** 419.
38. Sheldrick, G. M. SHELXS-97 and SHELXL-97,. *University of Gottingen,* **Germany, 1997**.
39. Bruker, B. A. I., SHELXTL Version 6.12,. *Madison, Wisconsin, USA,* **2001**.
40. X. Xiao, X. Han, Z. Mei, D. Zhu, K. Shao, J. Liang, M. Tian and L. Xu, *J. of Organomet. Chem.,* 2013, **729**, 28.
41. V. Chandrasekhar, K. Gopal, S. Nagendran, P. Singh, A. Steiner, S. Zacchini and J. F. Bickley, *Chem. Eur. J.,* 2005, **11**, 5437.
42. Z. Xu, C. Shen, Y. Hou, H. Gao and S. Sun, *Chem. Mater.,* 2009, **21**, 1778.
43. Y. Zhang, Y. Du, H. Xu and Q. Wang, *CrystEngComm,* 2010, **12**, 3658.

Phase-Pure Fabrication and Shape Evolution Studies of SnS Nanosheets

Malik Dilshad Khan, Javeed Akhtar, Mohammad Azad Malik, Masood Akhtar, and Neerish Revaprasadu

SnS nanosheets were synthesized by injection of n - *bis*(piperidinedithiocarbamato)tin(IV) in oleylamine at 230 °C.